Neuron, Vol. 15, 361–372, August, 1995, Copyright © 1995 by Cell Press

Characterization of a Novel Protein Regulated during the Critical Period for Song Learning in the Zebra Finch

Julia M. George, Hui Jin, Wendy S. Woods, and David F. Clayton
Department of Cell and Structural Biology
The Beckman Institute
The University of Illinois
Urbana, Illinois 61801

Summary

A male zebra finch learns a song by listening to a tutor, but song learning is normally restricted to a critical period in juvenile development. Here we identify an RNA whose expression in the song control circuit is altered during this critical period. The RNA encodes a soluble presynaptic protein that forms a predicted amphipathic α helix typical of the lipid-binding domain in apolipoproteins. We show this protein, which we call synelfin, to be the homolog of the human non-Aβ component (and its precursor) recently purified from Alzheimer's disease amyloid. We suggest this highly conserved protein may serve a novel function critical to the regulation of vertebrate neural plasticity.

Introduction

To carry out its functions, the brain must establish an extraordinary array of precise synaptic connections and then modulate and modify them at appropriate times throughout the life of the organism. To learn more about these processes, we have been pursuing a molecular biological analysis of one outstanding model of regulated neural plasticity, avian song learning. Oscine songbirds are distinctive in that they learn to match their own vocalizations to a model provided by a conspecific tutor (Thorpe, 1958; Nottebohm, 1968; Marler and Peters, 1977). In many species, the experience of hearing another bird can influence the individual's own vocal behavior only during a narrow window in juvenile development, a critical period for song learning (Nottebohm, 1968; Immelmann, 1969; Eales, 1985). Plastic changes in singing behavior are mirrored by physical changes in the anatomical circuit that controls song production (Nottebohm, 1981; Konishi and Akutagawa, 1985; Herrmann and Arnold, 1991). This "song control circuit" is composed of discrete nuclei, found primarily in the forebrain (see Figure 1), that apparently evolved for the explicit purpose of controlling learned song (Nottebohm et al., 1982; Brenowitz, 1991; Gahr et al., 1993).

The critical period for song learning is especially amenable to laboratory analysis in the zebra finch, where it proceeds through two overlapping phases (Immelmann, 1969). First, a young male forms an auditory model of a song presented to it by a tutor (usually its father), beginning as early as 20 days after hatching (Arnold, 1975). When birds are reared in open aviaries, song model acquisition is probably complete by about 35 days (Böhner, 1990). As the initial phase of song model acquisition closes, the young bird starts to rehearse the production of this song, beginning with very crude vocalizations at 25–30 days. The song reaches a relatively consistent adult form at about 60 days and finally becomes invariant and fully "crystallized" in the adult (~90 days; Arnold, 1975). The mechanisms that determine the opening and closing of the different phases of song learning are not known, but the apparent influence of gonadal steroid hormones on the process (Arnold, 1992) is consistent with a mechanism that involves specific gene regulation.

Among the nuclei that comprise the song control circuit, a direct and specific role in song learning, as opposed to song production, has been most clearly demonstrated for the lateral magnocellular nucleus of the anterior neostriatum (lMAN) and its afferents in the recursive loop of the song circuit (Bottjer et al., 1984; Scharff and Nottebohm, 1991; Morrison and Nottebohm, 1993). If a lesion is placed in lMAN in a young bird during the period of song model acquisition or early in the period of song rehearsal (before 50–60 days), the bird develops an abnormal song. However, the same lesion made in an adult has little effect on the bird's ability to produce a song already learned. lMAN sends its only efferent projection to the robust nucleus of the archistriatum (RA), which is the major output nucleus of the telencephalic song control circuit (Figure 1). RA also receives inputs from the high vocal center (HVC) in the neostriatum. In contrast to lMAN, both HVC and RA are necessary for ongoing song production (Bottjer et al., 1984; Scharff and Nottebohm, 1991), and the synapses from HVC to RA do not begin to form until 25 days or later, after the bird has begun to acquire a song model and as it begins to sing (Konishi and Akutagawa, 1985; Mooney and Rao, 1994). Since lMAN shows physiological responses to song stimuli (Doupe and Konishi, 1991) and is synaptically functional from the earliest stages of song acquisition (Mooney, 1992; Johnson and Bottjer, 1994; Mooney and Rao, 1994), it has been commonly suggested that the lMAN projection to RA may provide the mechanism by which the memory of the tutor song selectively entrains activity in the HVC–RA pathway so that vocal output comes to match the tutor song (reviewed in Doupe, 1993).

In this report, we describe the first gene to emerge from our studies of these phenomena (Clayton et al., 1988; Collum et al., 1991; George and Clayton, 1992; Mello and Clayton, 1994; Nastiuk et al., 1994; Nastiuk and Clayton, 1995) as a target of dynamic regulation during the critical period for song learning. The sequence was originally isolated in an experiment using differential hybridization techniques to identify RNAs regulated in the song circuit of canaries (George et al., 1993, Soc. Neurosci., abstract; see also George and Clayton, 1992). In adult songbirds, the gene shows a striking pattern of expression: it is generally abundant throughout the forebrain, but virtually absent in several key song control nuclei. In this report, we first show that this pattern of expression changes during early phases of the critical period for song learning in zebra

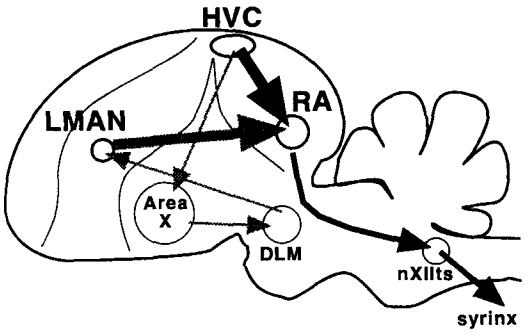

Figure 1. Schematic Representation of the Song Control Circuit in a Sagittal Section

The motor pathway for song production is shown in black, while the accessory pathway, or recursive loop, is shown in gray. Area X, a nucleus in the lobus parolfactorius; DLM, medial nucleus of the dorsolateral thalamus; HVC, high vocal center; IMAN, lateral magnocellular nucleus of the anterior neostriatum; nXIIts, tracheosyringeal portion of the hypoglossal nucleus, which innervates the muscles of the syrinx; RA, robust nucleus of the archistriatum.

finches. We then present a detailed characterization of the encoded protein. On the basis of this characterization, we named the protein synelfin, where "syn" indicates a local enrichment in synaptic terminals and "elf" (from the German for 11) refers to an extended organization of its primary structure around a distinctive 11 amino acid periodicity. Independent of our work on synelfin in songbirds, apparent homologs of this protein have now been reported for several other species, including humans (see Figure 7). The human protein was recently shown to be the precursor of an intrinsic component of amyloid plaques in Alzheimer's disease (AD; Ueda et al., 1993). Thus, an unusual and highly structured synaptic protein is both regulated in a principal animal model of neural plasticity and implicated as a participant in a human disease in which neural plasticity dramatically fails.

Results

Regulation of Synelfin Expression in Adult and Juvenile Zebra Finch Brain

The synelfin gene is expressed at high levels throughout most of the forebrain of adult canaries and zebra finches, but expression is specifically reduced in the major song control nuclei as assessed by either in situ hybridization to measure the RNA (see below) or immunocytochemistry to measure the protein (Figure 2). The anatomical boundaries between the song nuclei and surrounding telencephalon are sharply defined by the synelfin labeling pattern, as shown for RA (Figure 2C) using immunocytochemistry and confocal microscopy.

To quantitate the expression of synelfin at different phases of song learning, we used the technique of in situ hybridization and measured the relative abundance of the RNA in specific nuclei of the song control system (Figure 3; Figure 4). Male zebra finches at each of several ages were analyzed: 15 and 25 days of age (at the beginning of the song model acquisition phase), 35 days (during the transition from song acquisition to vocal learning), 60 days (late in the vocal learning phase), and 110 days (after song crystallization). For each animal examined, sections were selected for in situ hybridization that contained the principal song control nuclei, as determined by reference to control Nissl-stained sections taken from the same brain. Quantitative data were generated by computer-aided densitometry of in situ hybridization film autoradiograms and then normalized to a set of density standards. After subtraction of film background, data were expressed as a ratio of the signal within each nucleus relative to the signal in the immediately surrounding brain region. The normalized ratios were averaged for all birds of the same age, and the resulting means and SEMs were plotted to generate a time course of relative gene expression in specific song nuclei (Figure 3).

The developmental time course of synelfin mRNA in IMAN, HVC, and RA is graphed in Figure 3A. In IMAN, synelfin expression is increased relative to surrounding neostriatum at 15 and 25 days, and then drops by 35 days to a level significantly lower than that of the surrounding area, remaining there into adulthood. Each of the 15- and 25-day-old groups has a mean distinct from those of all other groups, and the overall change in expression in IMAN is highly significant (ANOVA for all five groups; $n = 3$ birds per group, $p < .00001$ for the null hypothesis that all means are equal; 15 versus 25 days, $p < .05$; 25 versus 35 days, $p < .01$). There is no significant difference in the means for the synelfin signal in IMAN within the 35-, 60-, and 110-day-old groups. A different result is observed in HVC and RA. In these nuclei, at all ages examined, synelfin mRNA is consistently reduced compared with surrounding brain regions. At 15 days, when synelfin expression is highest in IMAN, the signal in HVC is at a contrasting minimum (ANOVA, 15-day-old HVC versus grouped 25- to 110-day-old HVC, $p < .01$). In RA, there is no statistically significant difference in the expression of synelfin at any of the ages examined.

Adjacent sections from each bird were also hybridized to probes for two other genes that show differential expression in song nuclei of adult birds (Figure 3B). HAT-14 (Siepka et al., 1994, Soc. Neurosci., abstract) encodes a forebrain-enriched, neuron-specific dendritic protein related to RC-3/neurogranin (Represa et al., 1990; Watson et al., 1990). GAP-43 (Jin et al., 1994, Soc. Neurosci., abstract) encodes the canary homolog of a well-characterized growth-associated protein known to be enriched in axons, developmentally regulated in some brain regions, and phosphorylated during long-term potentiation (Benowitz and Routtenberg, 1987). Neither of these RNAs shows a statistically significant change in expression in IMAN compared with surrounding neostriatum at any of the ages examined (Figure 3B).

Digitized images of representative sections hybridized to the synelfin probe are shown for birds aged 15 days (Figure 4A) and 35 days (Figure 4B). IMAN is visually apparent as a peak of high expression in the 15-day-old bird (Figure 4A) and as a hole in the 35-day-old bird (Figure 4B). In contrast, expression in all other visible brain regions

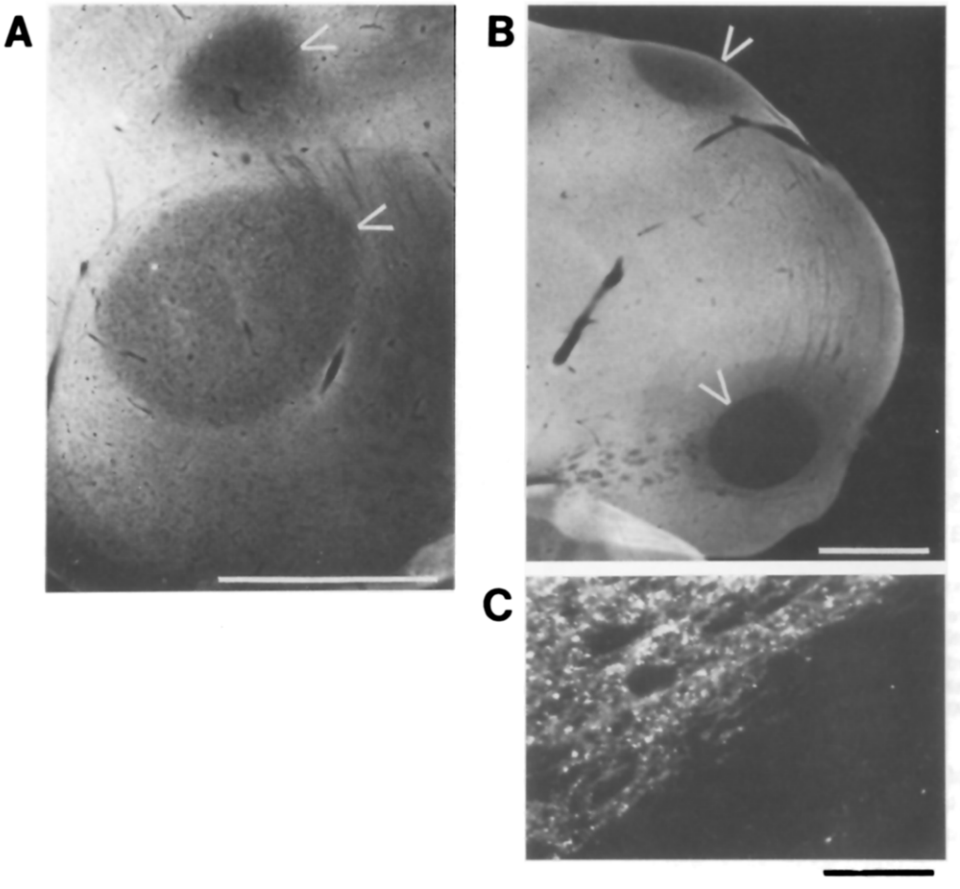

Figure 2. Selective Reduction in Synelfin Protein in Adult Zebra Finch Brain

(A) Low magnification micrograph illustrating the distribution of synelfin in a sagittal section of adult male zebra finch telencephalon, detected by immunofluorescence. This rostral field includes IMAN (upper arrowhead) and area X (lower arrowhead). Bar, 1 mm.

(B) Caudal telencephalon showing HVC (upper arrowhead) and RA (lower arrowhead). Bar, 1 mm.

(C) High magnification image using confocal microscopy to visualize immunofluorescence along the RA boundary (site corresponds to the tip of the lower arrowhead in [B]; 1 μm optical section thickness). Bar, 20 μm.

is essentially identical at these two ages. To confirm that the differences in hybridization signal are indicative of changes in cellular RNA levels, as opposed to nonspecific binding of the probe by tissue, representative sections were also analyzed by emulsion autoradiography (Figures 4C and 4D). In birds at 15 or 25 days, the large magnocellular neurons characteristic of IMAN are densely covered with autoradiographic silver grains (Figure 4C). In birds 35 days or older, these large neurons show little labeling above background levels (Figure 4D). We conclude that a large change in the expression of synelfin, but not at least two other genes encoding neuritic proteins, occurs in the magnocellular neurons of IMAN between 15 and 35 days of age.

Subcellular Localization of Synelfin Protein

Using confocal microscopy to visualize a thin optical section, the immunocytochemical staining pattern in the telencephalon is characterized by a punctate labeling that appears to exclude cell bodies and nuclei (see Figure 2C). The punctate labeling is abolished by preincubation of the antibody with the immunizing peptide (data not shown). A similar punctate quality of labeling has been described for antibodies to several proteins localized to presynaptic terminals, including synaptotagmin (Wendland et al., 1991), synapsin (de Camilli et al., 1983), and synaptophysin (Wiedenmann and Franke, 1985).

To define the localization of synelfin protein more precisely, we analyzed the distribution of synelfin protein in the zebra finch cerebellum, where cell bodies and processes are organized into three discrete layers (Figure 5). Sections were double labeled with antibodies to synelfin and synaptotagmin, a well-characterized integral membrane protein of synaptic vesicles (Matthew et al., 1981; Trimble et al., 1991). The anti-synaptotagmin antibody (red) gives bright, punctate staining of the molecular layer (Figure 5A), which contains few cells but is dense with presynaptic terminals arising from neurons in the granule cell layer. When the same section is visualized so that the signal from the anti-synelfin antibody is simultaneously visible (green), the punctate pattern of labeling in the molecular layer now appears a bright yellow (Figure 5B), indi-

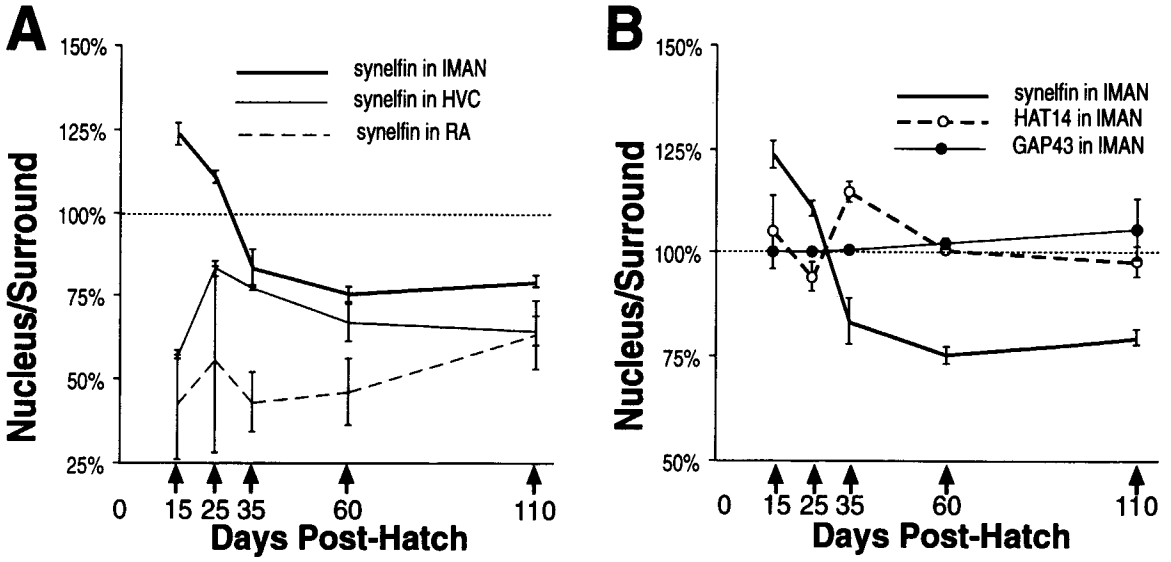

Figure 3. Selective Changes in Synelfin RNA Levels during the Critical Period for Song Development in Zebra Finches

(A) Synelfin RNA levels were measured within IMAN (thick line), HVC (thin line), and RA (dashed line) and expressed as ratios relative to the corresponding RNA level in the telencephalon surrounding each nucleus, as described in Results and Experimental Procedures. For each nucleus, means and SEMs for the birds in each age group are plotted.

(B) RNA levels in IMAN are shown for synelfin (same data as in [A]), HAT-14 (dashed line, open circles), and GAP-43 (thin line, solid circles). See Results for description of HAT-14 and GAP-43 probes. SEM bars are present on all data points, even when too small to be visible.

cating a close overlap of the synelfin and synaptotagmin signals in the molecular layer. Although the overlap is significant, it does not appear to be absolute, as close inspection shows discrete red and green spots, along with the more numerous yellow spots of double labeling. The anti-synelfin antibody does not react appreciably with Purkinje cell bodies, although some spots of labeling can be observed around the perimeter of these large neurons (Fig-

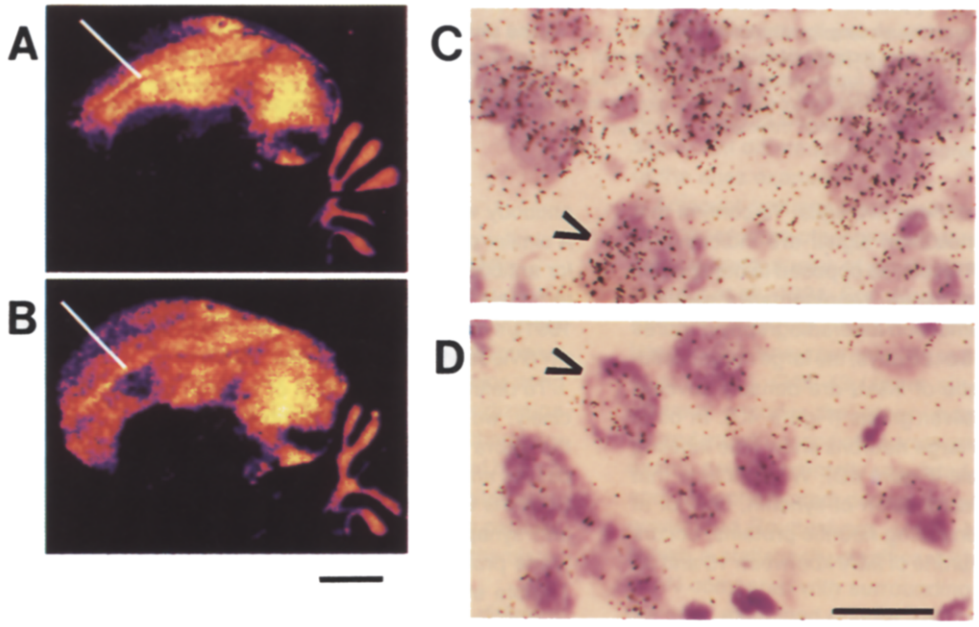

Figure 4. In Situ Hybridization Autoradiograms Showing Synelfin Regulation in IMAN

(A and B) Digitized X-ray film images, displayed using the Fire-2 color table of NIH Image. The diagonal white line indicates the location of IMAN, which is visible as a circle of high signal (yellow) in the 15-day-old bird (A) and a region of low signal (purple) in the 35-day-old bird (B). RA can also be seen (at the ventral posterior edge of the telencephalon) as an oval region of very low signal at both ages. Bar, 2 μm.

(C and D) Microscopic fields within IMAN after emulsion autoradiography and counterstaining with cresyl violet. Representative cells with the morphology of magnocellular neurons are indicated by arrowheads, for sections from birds at 15 (C) and 60 (D) days after parallel in situ hybridization and equal autoradiographic exposures. Bar, 20 μm.

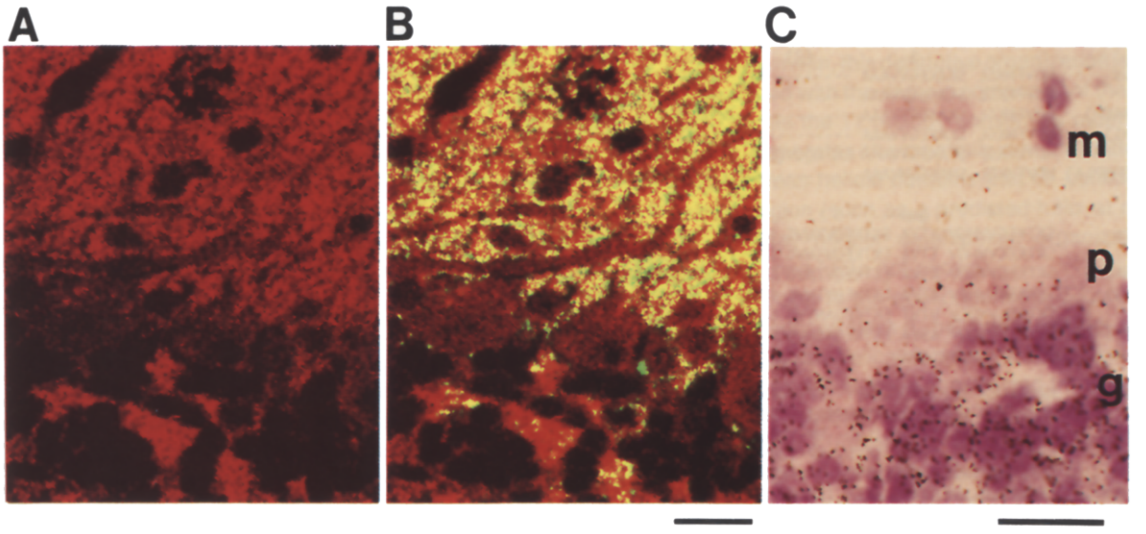

Figure 5. Presynaptic Localization of Synelfin Protein in Zebra Finch Cerebellum

(A) Synaptotagmin immunoreactivity in a section of zebra finch cerebellum (sagittal plane) detected by confocal microscopy (1 μm optical section thickness).

(B) Simultaneous display of synaptotagmin (red) and synelfin (green) immunoreactivity in the same section as in (A). A yellow signal appears wherever synaptotagmin and synelfin are closely colocalized. Bar, 20 μm.

(C) Comparable cerebellar field that has been hybridized for synelfin mRNA, exposed to autoradiographic emulsion, counterstained with the Nissl stain cresyl violet, and visualized by light microscopy. g, granule cell layer; m, molecular layer; p, Purkinje cell layer. Bar, 20 μm.

ure 5B). The anti-synelfin antibody also does not react with the cell bodies of granule neurons, although some apparent staining of the large glomerular synapses in the granule cell layer is present (Figure 5B).

This pattern of labeling (Figure 5B) is highly suggestive of a synaptic localization for synelfin, but on its own does not allow a discrimination between pre- and postsynaptic sites. Such a dense immunoreactivity in the molecular layer (Figure 5B) could represent either postsynaptic sites on Purkinje cell dendrites or the axonal endings of neurons whose cell bodies lie in the granular layer. We therefore determined which cells were responsible for synelfin synthesis by using in situ hybridization and emulsion autoradiography to localize synelfin RNA in similar sections in the cerebellum (Figure 5C). This shows that the synelfin RNA is present exclusively in the granule cell layer (Figure 5C). These data provide compelling evidence that, in the cerebellum, the synelfin protein is synthesized by granule neurons and transported out to their presynaptic axon terminals in the molecular layer. Consistent with a presynaptic localization of synelfin protein, we have also observed bright punctate labeling in cultured rat hippocampal neurons that colocalizes with synapsin I and synaptophysin immunoreactivity (Withers et al., 1994, Soc. Neurosci., abstract).

The resolution of confocal imaging is insufficient to determine whether or not synelfin is actually present in synaptic vesicles. To gain further insight into the subcellular distribution of the protein, we analyzed fractionated brain extracts by immunoblotting (Figure 6). The anti-synelfin antibody reacts with a band in zebra finches having the same apparent mobility (~20 kDa) as the recombinant protein expressed in bacteria (Figure 6A). A band of similar size is also detected in rat brain extracts (Figure 6A), and

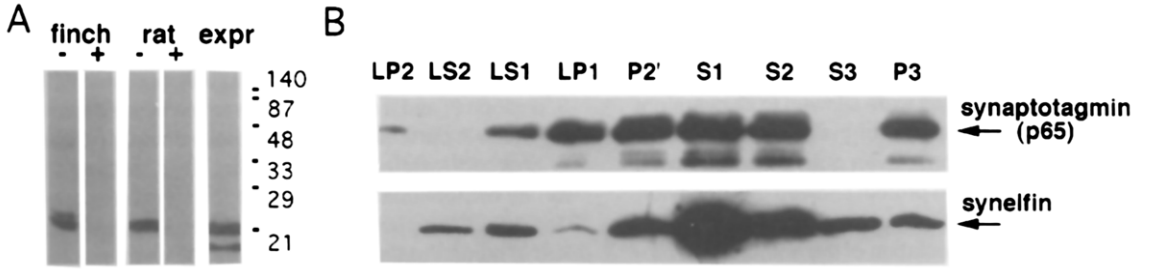

Figure 6. Immunoblot Analysis of Zebra Finch and Rat Brain Extracts Using Antibodies to the Synelfin C-Terminus

(A) Lanes 1–4 contain 20 μg of finch or rat proteins (S2 fraction; see Experimental Procedures) blotted and probed with a monoclonal antibody to the synelfin C-terminus, which has been preabsorbed with either a control peptide (–) or the immunizing peptide (+). Lane 5 contains synelfin peptide as expressed in E. coli after cleavage of exogenous residues (see Experimental Procedures).

(B) Subcellular fractions of zebra finch forebrain, as designated in Experimental Procedures; 0.5% of each fraction was electrophoresed, blotted, and probed with antibodies to either synaptotagmin (upper panel) or synelfin (lower panel).

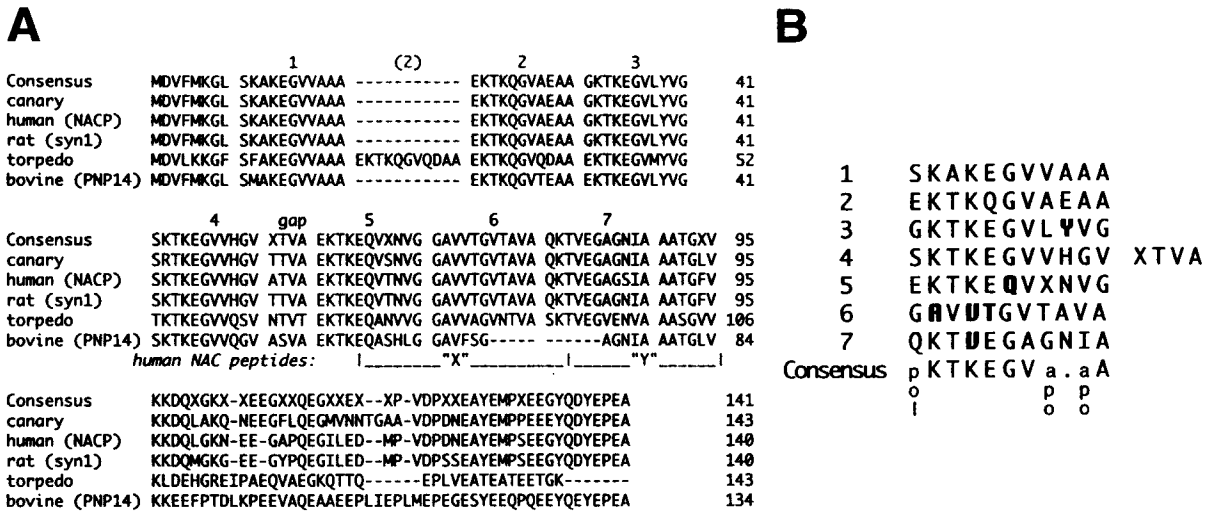

Figure 7. Sequence Conservation among Birds, Fish, and Mammals

(A) Alignment of peptide sequences from cDNAs of canary synelfin, human NACP, rat synuclein 1, and Torpedo synuclein, and as determined directly for the bovine PNP14 protein (see text). Each 11 residue repeat is set apart and numbered; the only break in the 11 residue periodicity is labeled "gap." The locations of the human X and Y peptides biochemically purified from AD amyloid (Ueda et al., 1993) are indicated. Residues included in the consensus at top occur in at least three of the five species.

(B) Alignment of the 11-residue repeats, using the consensus sequence derived for each numbered unit in (A). An overall consensus for the 11-mer is derived at the bottom. Within each numbered unit, residues that display a significantly different chemical character from the overall consensus and are conserved in all species are shown in boldface. apo, apolar residue; pol, polar residue.

preabsorption of the antibody with the immunizing peptide abolishes the reactivity in both species (Figure 6A, positive lanes). Brain extracts from rat (data not shown) or zebra finch were centrifuged to generate fractions representing crude cytosol (S2) or synaptosomes (P2′), and similar levels of synelfin were detected in both fractions (Figure 6B, lower panel). This distribution is similar to that observed for several synaptic vesicle–associated proteins (Huttner et al., 1983; Jahn et al., 1985). However, in contrast to the sedimentation behavior of synaptic vesicle–associated proteins, additional high speed centrifugation of the S2 fraction did not result in complete sedimentation of the cytosolic synelfin (compare S3 and P3 [Figure 6B, lower panel] and contrast with the distribution of synaptotagmin [upper panel]). Furthermore, when the P2′ pellet was diluted with water to lyse the synaptosomes, the majority of synelfin was released into the soluble fraction (LS1). Even after further centrifugation sufficient to sediment synaptic vesicles and synaptotagmin (LP2, upper panel), the synelfin released by lysis of synaptosomes remained in the soluble fraction (LS2, lower panel). We did observe evidence of a tendency of synelfin to precipitate out of solution: when homogenates were allowed to sit overnight prior to further fractionation, all of the synelfin was then found in particulate fractions. Even purified preparations of the bacterially expressed protein showed this behavior. This tendency to precipitate may account for previous assertions of membrane association of the homologous protein in other species, based on detection in particulate fractions (Maroteaux et al., 1988; Shibayama-Imazu et al., 1993). The results here (Figure 6) demonstrate instead that synelfin exists primarily as a soluble protein, despite its evident enrichment in axons and presynaptic terminals (see Figure 5).

The Synelfin Peptide Sequence

The deduced synelfin protein is presented in Figure 7A, where it is aligned with largely identical sequences that subsequently appeared in GenBank, representing human (Ueda et al., 1993), rat (Maroteaux and Scheller, 1991), bovine (Nakajo et al., 1993), and the electric fish Torpedo (Maroteaux et al., 1988). General features of the amino acid sequence conserved in all species include a similar overall size of 134–143 residues, a high lysine:arginine ratio, a complete absence of cysteines and tryptophans, and an acidic C-terminal domain. The first 89 residues are composed almost entirely of variants of a degenerate 11 amino acid consensus motif, derived in Figure 7B. With certain exceptions (discussed below), this motif is repeated seven times in each sequence. Despite the recognizeable similarities among the repeating 11-residue units, each repeating unit has a unique signature: a set of exceptions from the consensus that distinguishes it from the other repeats and that has been conserved among all the species compared (Figure 7B, boldface). The conserved variations from the consensus include the presence of a tyrosine residue in all sequences at only one position (unit 3, position 9) and a conserved glutamine in unit 2 (position 5). Unit 6 is particularly notable for the complete absence of charged residues in all species, thus defining a uniformly hydrophobic stretch within the synelfin sequence. The non-Aβ component (NAC) peptide purified from amyloid in human brains (Ueda et al., 1993) includes this portion of the sequence (Figure 7A). The 11 residue periodicity is broken once in all species, by the insertion of 4 uncharged amino acids separating units 4 and 5.

Species-specific deletions or insertions underscore the apparent structural significance of the overall 11 residue periodicity. The Torpedo sequence (Figure 7A) bears an

exact in-frame duplication of the second 11 residue repeat. In the bovine PNP14 sequence (Figure 7A), an 11 amino acid deletion straddles units 6 and 7, removing the N-terminal hydrophilic residues of unit 7 so that the fused sequence still bears the distinctive apolar character of unit 6. Finally, an alternative human form (data not shown) has recently been reported (Jakes et al., 1994) that contains a similar 11 residue deletion that preserves the hydrophobicity of unit 6, yet that deletion is shifted by 1 residue relative to the site of the bovine PNP14 deletion. Thus, each of these three changes has precisely conserved the 11 residue periodicity.

The remaining sequence is consistently hydrophilic and acidic in all species, with a preponderance of glutamate residues over aspartates. Visual inspection of Figure 7A shows that the sequences from canary, human (NACP), and rat (synuclein 1) share an especially high level of specific identity in this domain. Bovine PNP14 has a C-terminal domain that is slightly different in its precise sequence but chemically similar in its general features (e.g., note the abundance of glutamate residues). Homologous rat and human variants have been detected that share this alternative PNP14 C-terminal sequence (Tobe et al., 1992; Jakes et al., 1994). We have so far not observed evidence for such a variant in birds. Both forms of the protein, in all species except Torpedo, end with the C-terminal consensus EGYQDYEPEA.

Helical Wheel Analysis of Secondary Structure

The most unusual and highly conserved feature of this protein sequence thus appears to be its organization around an underlying 11 residue repeating motif. Such a motif has been described in two other classes of proteins of which we are aware: the exchangeable apolipoproteins (A-I, A-II, A-IV, C-I, C-II, C-III, and E; reviewed in Segrest et al., 1992) and a group of plant proteins that accumulate to very high levels during desiccation and seed formation (reviewed in Dure, 1993). Both of these other groups of proteins are believed to fold as α helices, and the conservation of the 11 residue periodicity has been suggested to reflect the particular constraints of imposing an additional amphipathic requirement onto an α-helical structure (since the rise of the α helix is approximately 3.6 residues per turn, every 11th residue will line up on the same side of the helix within 20 degrees, facilitating an extended separation of polar and apolar faces; see Segrest et al., 1990). We therefore examined whether the 11 residue motif in synelfin might confer a similar amphipathic α-helical conformation.

Algorithms for analysis of secondary structure predict that residues 9–35, 52–63, and 88–103 of synelfin are likely to form an α helix (data not shown), so we constructed helical wheel displays to observe where each of these residues would fall relative to the long axis of the helix (Shiffer and Edmundson, 1967). A representation of the first 18 helical residues of canary synelfin (9–26; identical also in human NACP and rat synuclein) is shown in Figure 8A and demonstrates clear amphipathic segregation of polar and apolar residues to opposite faces of the predicted helix. Moreover, there is a precise clustering of 2 basic residues (lysine) at each polar–apolar interface and acidic residues (glutamate) at the center of the polar face. Within synelfin, this distinctive organization is specifically associated with the domain composed of the 11 residue repeats, as the 11 residue consensus motif derived in Figure 7B generates an essentially identical pattern (Figure 8B), whereas helical domains that lie outside of the 11 residue region (such as a predicted helix at residues 88–103) display neither amphipathic organization nor charge clustering (data not shown).

For comparison to the apolipoproteins, Figure 8C displays the consensus class A_2 helix derived from an analysis of eight separate helical domains in the apolipoproteins A-II, C-I, C-II, and C-III (helix constructed from the data in Figure 10B of Segrest et al., 1992). This helical motif has been considered a unique and defining characteristic that distinguishes the lipid-binding domain from other helical domains within apolipoprotein or in other helix-forming proteins (Segrest et al., 1990). Note that the charge distribution is virtually superimposable upon that observed in synelfin (Figures 8A and 8B), including the following specific points of similarity: the apolar face has the same extent (8 residues; closed circles), the polar–apolar junction on each side is demarcated by the presence of 2 lysines, and the central positions on the polar face are occupied by glutamate. In Figure 8D we present a helical wheel derived from the consensus 11 residue motif in the plant desiccation proteins (Dure, 1993); intriguingly, the pattern of charge clustering is generally similar, although the size

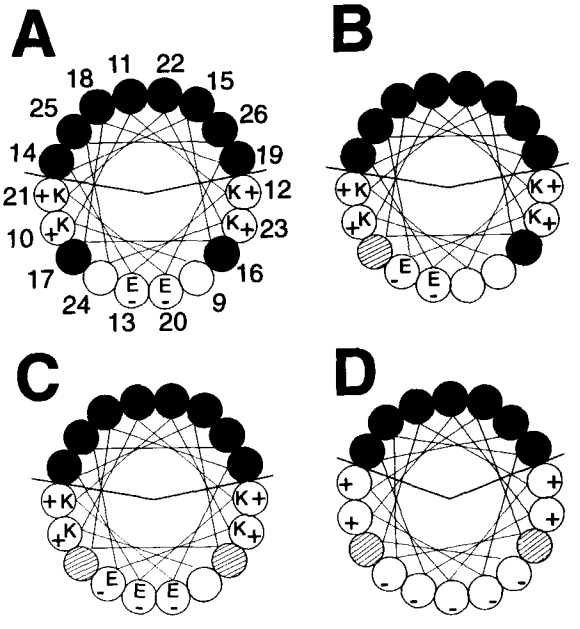

Figure 8. Helical Wheel Comparison of Synelfin, Apolipoprotein, and LEA76

(A) Canary synelfin, residues 9–26 (identical to human and rat); (B) synelfin, 11-mer consensus sequence derived in Figure 7B; (C) apolipoprotein, class A_2 helix (Segrest et al., 1992); (D) LEA76, 11-mer consensus sequence (Dure, 1993). Apolar residues are shown in black (following the convention that glycine and threonine are considered hydrophobic when they occur on the hydrophobic face), and charged residues are indicated by plus or minus sign.

of the apolar face is smaller by 1 residue, and the negative cluster in the center of the polar face is larger than that observed in synelfin or apolipoprotein.

Discussion

Here we have described the discovery and characterization of a gene regulated in the avian song control circuit during the critical period for song learning. We observed a significant change in synelfin gene expression during early stages of song learning in one key nucleus, IMAN, primarily between 25 and 35 days of age (see Figure 3; Figure 4). At the beginning of this period, synelfin mRNA in IMAN is more abundant than in the surrounding neostriatum; by the end it has dropped to a much lower level, where it remains into adulthood. A more subtle change in synelfin expression in HVC is also indicated by our data (Figure 3A), although this change is difficult to interpret given the diversity of neuronal subtypes in HVC and the potential impact of neuronal turnover within this particular nucleus (Nordeen and Nordeen, 1990; Bottjer and Johnson, 1992). The significance of synelfin regulation in IMAN is underscored by the lack of regulation in this nucleus for two other genes that, like synelfin, encode proteins found in the cytosol of neurites (GAP-43 and HAT-14; see Figure 3B).

As our quantitative measurements (see Figure 3) are expressed as ratios, the observed change in synelfin ratio in IMAN could in principle reflect either a selective decline in synelfin mRNA within IMAN or a selective increase within the surrounding forebrain. The latter possibility is effectively excluded by the lack of parallel changes in the ratio for synelfin in two other song nuclei in the nearby forebrain (see Figure 3A), the lack of any change in the expression ratios for two other genes in IMAN (see Figure 3B), the overall stability of the hybridization pattern in the rest of the brain (see Figures 4A and 4B), and evidence derived from emulsion autoradiography of individual cells (see Figures 4C and 4D). Furthermore, RNA blot analysis indicates that synelfin RNA levels are relatively stable in the forebrain as a whole after about 14 days of age (H. J., J. M. G., and D. F. C., unpublished data). We conclude that the change in synelfin ratio in IMAN (see Figure 3) is primarily an indication of a selective decline in synelfin mRNA within IMAN between 25 and 35 days of age. Consistent with this change in RNA levels and with the presynaptic localization of the protein, we also observed that the immunocytochemical signal for synelfin protein in RA (the nucleus to which IMAN neurons project) is notably higher in young birds than in adults (data not shown).

Since synelfin is a presynaptic protein (see Figure 5), this change in synelfin gene expression in IMAN could be related to a structural change in presynaptic terminals from IMAN onto RA that has been shown to occur at a similar time: the terminals double in size while their number decreases by half, in comparisons of birds at 25 versus 53 days of age (Herrmann and Arnold, 1991). As the number of neurons projecting from IMAN to RA appears to be stable after 25 days (Nordeen et al., 1992), these data suggest that a rearrangement of IMAN synapses onto RA is occurring during the same time in which synelfin gene expression in IMAN is declining. Other biochemical changes observed in IMAN during this general period include an increase in MK-801 binding within IMAN's borders at 30 days relative to adults, indicative of an increased concentration of N-methyl-D-aspartate receptors within IMAN (Aamodt et al., 1992), and a decreased level of androgen binding in IMAN at 25 days relative to 60 days (Bottjer, 1987). It seems unlikely that the drop in synelfin during this period is simply a general consequence of neuronal maturation, since synelfin RNA and protein levels remain high throughout most of the rest of the telencephalon in adult birds (see Figure 2; Figure 4B). Furthermore, IMAN's afferent inputs (Johnson and Bottjer, 1994) and efferent outputs (Mooney and Rao, 1994) are both present by day 15. Expression of synelfin thus continues at a high level for approximately 2 weeks beyond the initial establishment of IMAN's synaptic connections, before it selectively drops in IMAN while remaining constant in the rest of the forebrain.

These biochemical and morphological changes in IMAN neurons could conceivably contribute to either or both of the following behavioral phenomena: the age-limited acquisition of a primary song model, which under normal rearing conditions may be complete by day 35 (Böhner, 1990); and the beginning of the period of motor learning, which normally occurs around day 30 (Immelmann, 1969; Arnold, 1975). If synelfin gene regulation in IMAN has a causal role in the functional changes associated with song acquisition, then manipulation of synelfin expression in IMAN during the critical period should have an effect on song development. While carrying out such an experiment is not trivial, the high degree of anatomical definition in the song circuit may make it a favorable system for exploring the targeted delivery and expression of specific genetic constructs. Alternatively, behavioral and hormonal manipulations that alter the process of song development might be expected to influence synelfin gene expression, although failure to see such effects would not disprove a significant causal role for synelfin regulation in the normal process of song acquisition. Treatments that have been reported to alter song development include early administration of testosterone, which may cause premature closure of the critical period (Sossinka et al., 1975; Korsia and Bottjer, 1991), and isolation of young birds away from potential song tutors, which may delay closure of the critical period (Eales, 1985; Morrison and Nottebohm, 1993). Experiments are in progress to measure synelfin regulation in each of these paradigms (Jin and Clayton, 1995, Soc. Neurosci., abstract).

The gene we have identified as regulated during the development of the song control system encodes an unusual and highly conserved brain-specific protein abundant in the mature vertebrate telencephalon. Full appreciation of its degree of conservation and its precise sequence organization has come only with the parallel identification of related sequences in fish, rodents, cows, and humans. A similar protein was described by Maroteaux et al. (1988), who first cloned it from the electric eel Torpedo, and then from rat brain (Maroteaux and Scheller,

1991). Although these workers originally referred to the protein as synuclein, to indicate its apparent presence in both synapses and cell nuclei, no confirmatory evidence of nuclear localization has appeared since the first publication. Nakajo and colleagues independently identified the same or a closely related protein in bovine and rat brain extracts (Nakajo et al., 1990; Tobe et al., 1992) and used electron microscopy to detect the protein in presynaptic endings in the cerebellum and telencephalon, but it was not directly associated with either synaptic vesicles or the cell nucleus (Nakajo et al., 1990, 1994). Subsequently, they also showed it to be a phosphoprotein (Nakajo et al., 1993) and termed it PNP14 (phosphoneuroprotein-14 kDa molecular weight). Even more recently, related sequences were independently isolated from human brain by two different labs (Ueda et al., 1993; Jakes et al., 1994), and antibodies to the protein were used to demonstrate a specific presynaptic localization in rat brain (Iwai et al., 1995).

Our own data show clear evidence that the homologous protein in songbirds is enriched in axons and presynaptic terminals (see Figure 3; Figure 4) and relatively abundant in preparations of synaptosomes (see Figure 5). Our immunocytochemical studies of both finch (see Figure 3; Figure 4) and rat (unpublished data) provide no evidence for specific labeling of cell nuclei, i.e., labeling that is not abolished by preincubation of antisera with immunizing peptide. Our data demonstrate conclusively that the protein exists in a soluble form both in the cytosol and in synaptosomes (see Figure 5), although it shows a propensity to precipitate out of solution over time. Despite the protein's lack of tight association with synaptic vesicles or membranes, it nonetheless comes to be enriched at synaptic terminals. The decreased abundance of the protein in HVC, RA, IMAN, and area X (see Figure 2) is consistent with a presynaptic localization: the major inputs to these nuclei come exclusively (for RA, IMAN, and area X) or partly (for HVC) from other song nuclei or thalamic regions where levels of synelfin mRNA are low. Studies to characterize the mechanism of this presynaptic localization might provide insight into the molecules or structures with which synelfin interacts, and hence into its function.

Our structural analysis of the conserved peptide sequence reveals a strong relationship to the apolipoproteins and, in particular, their lipid-binding domains (see Figure 8). The lipid-binding amphipathic α helices of apolipoproteins have been subjected to intense experimental and theoretical analysis, out of which has emerged a model of the way in which they associate with phospholipids (Segrest et al., 1974, 1992). The apolar face (Figure 8C) is believed to interact with the hydrophobic tails of phospholipids, possibly even in biological lipid bilayers (LeBlond and Marcel, 1991; Segrest et al., 1992). The paired lysine residues at each polar–apolar interface have been suggested to allow a "snorkeling" effect that buries the apolar face deeper within the hydrophobic lipid environment, while the negatively charged glutamate residues on the center of the polar face form stable interactions with the charged phospholipid head groups (Segrest et al., 1974, 1992). The presence of a similar structure in synelfin should allow an interesting test of whether these specific sequence features are necessary or sufficient to mediate specific lipid interactions.

Despite the remarkable resemblance to apolipoproteins, synelfin is different from apolipoprotein in several significant ways and may have entirely different functions. Apolipoprotein is a secreted molecule, whereas synelfin appears to be primarily an intracellular molecule. Evidence for this includes the lack of defined signal sequences for import into the endoplasmic reticulum, immunocytochemical staining patterns in primary cultures of finch neurons and rat hippocampal neurons (G. Withers and J. M. G., unpublished data), and our inability so far to detect it in cerebrospinal fluid (data not shown). A second major difference from the apolipoproteins is the conservation of specific residues at most positions throughout the synelfin sequence; in the apolipoproteins, an overall amphipathic organization is maintained with little conservation of specific residues (Boguski et al., 1985; Segrest et al., 1992). A third difference is the presence in synelfin of a second, apparently unrelated, highly acidic and mostly nonhelical C-terminal domain.

Two independent reports have recently implicated the human synelfin homolog in AD. Ueda et al. (1993) obtained peptide sequence from a previously uncharacterized intrinsic component of AD plaque amyloid (retained in amyloid through SDS purification). They termed it NAC (for non-Aβ component, to distinguish it from Aβ, the other major intrinsic component of amyloid), and the cloned NAC precursor protein was termed NACP. Antibodies against the NAC peptides reacted specifically with extracellular amyloid plaques in AD brain tissue sections (Ueda et al., 1993). Even more recently, Jakes et al. (1994) independently discovered this same human protein, using an antibody originally raised against paired helical filament cores extracted from neurofibrillary tangles in AD neurites. They also found evidence for another form in humans more similar to rat PNP14 (Nakajo et al., 1993). Our own observation here of a structural relationship to the exchangeable apolipoproteins raises yet one more speculative link to AD, as the ε4 allele of the apolipoprotein E gene has recently been shown to predispose its bearers to the development of late onset AD (Corder et al., 1993). Studies of the biochemistry and cell biology of this intriguing protein promise to shed light on processes that contribute to the regulation of neural plasticity, and perhaps also to the devastating pathology of AD.

Experimental Procedures

Cloning and DNA Sequence Analysis

A cDNA library was constructed in the vector λgt10 from RNA extracted from the HVC-associated telencephalon (HAT) of adult male canaries (in March of 1986), and screened by standard differential hybridization methods (Clayton et al., 1988) for clones of RNAs more abundant in the HAT region compared with the hindbrain–midbrain region (George and Clayton, 1992). The synelfin cDNA was originally identified as clone HAT-3; the cDNA and deduced peptide sequences have been deposited in the GenBank database (accession number L33860). Structural analysis of peptide sequences was performed using the pSAAM software package developed by Anthony Crofts (Beckman Institute, University of Illinois).

In Situ Hybridization Analysis of Zebra Finches in the Critical Period

Zebra finches were bred and raised in a free-flight group aviary maintained under a 12:12 hr light–dark cycle at the Beckman Insititute, Urbana, IL. Frozen brain sections (10 μm) were hybridized to ^{35}S-labeled riboprobes using high stringency conditions followed by X-ray film or emulsion autoradiography, as described elsewhere in detail (Clayton et al., 1988; Clayton and Alvarez-Buylla, 1989). For hybridization of zebra finch sections with probes derived from canary cDNAs, the final wash was in 0.1 × SSPE at 65°C (see Clayton et al., 1988). Parallel hybridizations were performed with sense-strand controls for evaluation of nonspecific background levels, which were negligible in these experiments. All hybridizations were replicated on at least two separate occasions.

Identification of song nuclei on X-ray films was confirmed by microscopic inspection of counterstained sections following emulsion autoradiography, by inspection of stained reference sections from each brain, and by comparison of adjacent sections hybridized with the HAT-9 probe, which recognizes an abundant RNA that is selectively reduced in song nuclei at all ages (unpublished data). Film images were digitized on a high resolution flat-bed scanner and analyzed using NIH Image software (version 1.54) running on a Power Macintosh computer with a large monitor. Brain regions were traced, and the average optical density within each region was computed by reference to a calibrated Kodak step tablet digitized under identical conditions. For each section, the value for the adjacent film background was subtracted from all measurements, and then nucleus:surround ratios were calculated for all song nuclei represented on that section. The "surround" was defined for IMAN as the anterior neostriatum present on the same sagittal section; for HVC, as the caudal neostriatum; and for RA, as the archistriatum (because the archistriatum is a complex region with variegated gene expression, RA signals were first measured relative to the caudal neostriatum on the same section, and this ratio was then corrected by a factor representing the average ratio of synelfin signal in archistriatum versus caudal neostriatum, measured for all sections). The mean value for all ratio measurements of each nucleus in each bird was calculated, and this value for each bird was used to calculate group means and SEMs for each nucleus at each age (n = 3 birds per age). Single-factor ANOVA calculations were performed using Microsoft Excel. Histogram analysis of the collected data indicated normal distributions in the samples compared by ANOVA, and plots of means versus SDs did not reveal any systematic trend that would disqualify analysis by standard parametric tests.

Preparation of Anti-Peptide Antibodies

The C-terminal peptide CEMPPEEEYQDYEPEA was synthesized, conjugated to keyhole limpet hemocyanin, and purified by gel exclusion chromatography (Imject Activated Immunogen Conjugation Kit, Pierce). The University of Illinois Hybridoma Facility immunized mice, provided test sera (which were screened against the synelfin–maltose-binding protein fusion protein), and generated monoclonal fusions from positively reactive mice.

Immunocytochemistry of Brain Tissue

Brain tissue was fixed by intracardial perfusion with 3% neutral-buffered paraformaldehyde with 0.75 M lysine, 0.1 M sodium metaperiodate and embedded in polyethylene glycol as described (Clayton and Alvarez-Buylla, 1989). Sections (20 μm) were probed sequentially with primary antibody (H3 monoclonal [1:10,000], rabbit polyclonal antibody against p65 synaptotagmin [1:100; a gift from L. Elferink and R. Scheller]) and fluorescent secondary antibody (goat anti-mouse LRSC and goat anti-rabbit Cy5 [1:100; Jackson Immunochemicals]). To assess nonspecific immunoreactivity, antibodies were preincubated at 4°C overnight with either the immunizing peptide or a nonabsorbing control peptide (20 μg/ml). Digitized fluorescence data were collected on a Bio-Rad MRC 600 laser scanning confocal microscope.

Bacterial Expression of the Synelfin Peptide

Synelfin coding sequences were subcloned into the expression vector pMAL-c (New England Biolabs). This construct directed expression of a synelfin–maltose-binding protein fusion, which was purified by affinity chromatography on amylose resin and eluted with maltose. Exogenous residues were cleaved with the protease Factor Xa.

Immunoblot Analysis

A partial subcellular fractionation (Huttner et al., 1983) was performed on tissue representing zebra finch or rat forebrain. Forebrain tissues were homogenized in a glass-Teflon homogenizer in ~10 vol of ice-cold 0.32 M sucrose, 5 mM Tris (pH 7.5), 2.5 mM phenylmethylsulfonyl fluoride and centrifuged at 1000 × g for 5 min at 4°C. The supernatant (S1) was further centrifuged at 12,500 × g for 15 min at 4°C to generate a supernatant (S2) and a pellet (P2). The S2 supernatant was immediately centrifuged at 174,000 × g for 1 hr at 4°C, in a Beckman TL100 ultracentrifuge equipped with a TLA 100.3 rotor, to generate a cytosolic fraction (S3) and a pellet (P3). Meanwhile, the P2 pellet was washed and resuspended in homogenization buffer to give a crude synaptosomal fraction (P2′). The P2′ fraction was mixed with 10 vol of H_2O, subjected to five strokes with a glass-Teflon homogenizer, brought to 10 mM Tris (pH 7.5), and incubated on ice for 30 min with frequent mixing. This lysed synaptosomal preparation was then spun at 25,000 × g for 20 min, to yield a lysate pellet (LP1) and a lysate supernatant (LS1). The LS1 supernatant was subjected to further centrifugation at 174,000 × g for 2 hr at 4°C, to yield a supernatant (LS2) and a crude synaptic vesicle fraction (LP2).

Proteins were separated by SDS–PAGE (Laemmli, 1970) and electrophoretically transferred to nitrocellulose (Towbin et al., 1979). Blots were probed sequentially with primary (1:10,000–1:100,000) and secondary (horseradish peroxidase–linked sheep anti-mouse Ig; 1:3000; Amersham) antibodies and processed for enzyme-linked chemiluminescent detection, all as specified by the ECL Western Blotting Kit (Amersham). In some cases, primary antibody dilutions were preabsorbed with immunizing peptide or control peptides prior to use.

Acknowledgments

We thank Fernando Nottebohm for providing canaries, performing the initial preparative dissections in 1986, and lending support in numerous other ways; Maria Huecas for technical assistance; Richard Scheller and Lisa Elferink for providing anti-synaptotagmin antiserum; Christopher Wallace for rat brain extracts; the Cell Science Center Hybridoma Facility at the University of Illinois for production of monoclonal antibodies; William Greenough, Gene Robinson, Alan F. Horwitz, Gary Banker, Ginger Withers, and Brad Hyman for critical comments on early drafts of the manuscript; and Sandra Siepka and Telsa Mittelmeier for comments on the final draft. This work was supported by National Institutes of Health grants NS 25742 and HD 07333.

The costs of publication of this article were defrayed in part by the payment of page charges. This article must therefore be hereby marked *"advertisement"* in accordance with 18 USC Section 1734 solely to indicate this fact.

Received October 24, 1994; revised May 26, 1995.

References

Aamodt, S. M., Kozlowski, M. R., Nordeen, E. J., and Nordeen, K. W. (1992). Distribution and developmental change in [^{3}H]MK-801 binding within zebra finch song nuclei. J. Neurobiol. *23*, 997–1005.

Arnold, A. P. (1975). The effects of castration on song development in zebra finches (*Poephila guttata*). J. Exp. Zool. *191*, 261–278.

Arnold, A. P. (1992). Developmental plasticity in neural circuits controlling birdsong: sexual differentiation and the neural basis of learning. J. Neurobiol. *23*, 1506–1528.

Benowitz, L., and Routtenberg, A. (1987). A membrane phosphoprotein associated with neural development, axonal regeneration, phospholipid metabolism, and synaptic plasticity. Trends Neurosci. *10*, 527–532.

Boguski, M., Elshourbagy, N., Taylor, J., and Gordon, J. (1985). Comparative analysis of repeated sequences in rat apolipoproteins A-I, A-IV, and E. Proc. Natl. Acad. Sci. USA *82*, 992–996.

Böhner, J. (1990). Early acquisition of song in the zebra finch, *Taeniopygia guttata*. Anim. Behav. *39*, 369–374.

Bottjer, S. (1987). Ontogenetic changes in the pattern of androgen accumulation in song-control nuclei of male zebra finches. J. Neurobiol. *18*, 125–139.

Bottjer, S. W., and Johnson, F. (1992). Matters of life and death in the songbird forebrain. J. Neurobiol. *23*, 1172–1191.

Bottjer, S. W., Miesner, E. A., and Arnold, A. P. (1984). Forebrain lesions disrupt development but not maintenance of song in passerine birds. Science *224*, 901–903.

Brenowitz, E. A. (1991). Evolution of the vocal control system in the avian brain. Sem. Neurosci. *3*, 399–407.

Clayton, D. F., and Alvarez-Buylla, A. (1989). *In situ* hybridization using PEG-embedded tissue and riboprobes: increased cellular detail coupled with high sensitivity. J. Histochem. Cytochem. *37*, 389–393.

Clayton, D. F., Huecas, M. E., Sinclair-Thompson, E. Y., Nastiuk, K. L., and Nottebohm, F. (1988). Probes for rare mRNAs reveal distributed cell subsets in canary brain. Neuron *1*, 249–261.

Collum, R. G., Clayton, D. F., and Alt, F. W. (1991). Structure and expression of canary *myc* family genes. Mol. Cell. Biol. *11*, 1770–1776.

Corder, E., Saunders, A., Strittmatter, W., Schmechel, D., Gaskell, P., Small, G., Roses, A., Haines, J., and Pericak-Vance, M. (1993). Gene dose of apolipoprotein E type 4 allele and the risk of Alzheimer's disease in late onset families. Science *261*, 921–923.

de Camilli, P., Cameron, R., and Greengard, P. (1983). Synapsin I (protein I), a nerve terminal-specific phosphoprotein. I. Its general distribution in synapses of the central and peripheral nervous system demonstrated by immunofluorescence in frozen and plastic sections. J. Cell Biol. *96*, 1337–1354.

Doupe, A. (1993). A neural circuit specialized for vocal learning. Curr. Biol. *3*, 104–111.

Doupe, A. J., and Konishi, M. (1991). Song-selective auditory circuits in the vocal control system of the zebra finch. Proc. Natl. Acad. Sci. USA *88*, 11339–11343.

Dure, L. I. (1993). A repeating 11-mer amino acid motif and plant desiccation. Plant J. *3*, 363–369.

Eales, L. A. (1985). Song learning in zebra finches: some effects of song model availability on what is learnt and when. Anim. Behav. *33*, 1293–1300.

Gahr, M., Guttinger, H.-R., and Kroodsma, D. (1993). Estrogen receptors in the avian brain: survey reveals general distribution and forebrain areas unique to songbirds. J. Comp. Neurol. *327*, 112–122.

George, J. M., and Clayton, D. F. (1992). Differential regulation in the avian song control circuit of an mRNA predicting a highly conserved protein related to protein kinase C and the *bcr* oncogene. Mol. Brain Res. *12*, 323–329.

Herrmann, K., and Arnold, A. (1991). The development of afferent projections to the robust archistriatal nucleus in male zebra finches: a quantitative electron microscopic study. J. Neurosci. *11*, 2063–2074.

Huttner, W., Schiebler, W., Greengard, P., and de Camilli, P. (1983). Synapsin I (protein I), a nerve terminal-specific phosphoprotein. III. Its association with synaptic vesicles studied in a highly purified synaptic vesicle preparation. J. Cell Biol. *96*, 1374–1388.

Immelmann, K. (1969). Song development in the zebra finch and other estrilid finches. In Bird Vocalizations, R. A. Hinde, ed. (Cambridge, England: Cambridge University Press), pp. 61–74.

Iwai, A., Masliah, E., Yoshimoto, M., Ge, N., Flanagan, L., Rohan de Silva, H., Kittel, A., and Saitoh, T. (1995). The precursor protein of non-Aβ component of Alzheimer's disease amyloid is a presynaptic protein of the central nervous system. Neuron *14*, 467–475.

Jahn, R., Schiebler, W., Ouimet, C., and Greengard, P. (1985). A 38,000-dalton membrane protein (p38) present in synaptic vesicles. Proc. Natl. Acad. Sci. USA *82*, 4137–4141.

Jakes, R., Spillantini, M., and Goedert, M. (1994). Identification of two distinct synucleins from human brain. FEBS Lett. *345*, 27–32.

Johnson, F., and Bottjer, S. (1994). Afferent influences on cell death and birth during development of a cortical nucleus necessary for learned vocal behavior in zebra finches. Development *120*, 13–24.

Konishi, M., and Akutagawa, E. (1985). Neuronal growth, atrophy and death in a sexually dimorphic song nucleus in the zebra finch. Nature *315*, 145–147.

Korsia, S., and Bottjer, S. (1991). Chronic testosterone treatment impairs vocal learning in male zebra finches during a restricted period of development. J. Neurosci. *11*, 2362–2371.

Laemmli, E. K. (1970). Cleavage of structural proteins during the assembly of the head of bacteriophage T4. Nature *227*, 680–685.

LeBlond, L., and Marcel, Y. (1991). The amphipathic α-helical repeats of apolipoprotein A-I are responsible for binding of high density lipoproteins to HepG2 cells. J. Biol. Chem. *266*, 6058–6067.

Marler, P., and Peters, S. (1977). Selective vocal learning in a sparrow. Science *198*, 519–527.

Maroteaux, L., and Scheller, R. (1991). The rat brain synucleins: a family of proteins transiently associated with neuronal membrane. Mol. Brain Res. *11*, 335–343.

Maroteaux, L., Campanelli, J., and Scheller, R. (1988). Synuclein: a neuron-specific protein localized to the nucleus and presynaptic terminal. J. Neurosci. *8*, 2804–2815.

Matthew, W. D., Tsavaler, L., and Reichardt, L. F. (1981). Identification of a synaptic vesicle-specific membrane protein with a wide distribution in neuronal and neurosecretory tissue. J. Cell Biol. *91*, 257–269.

Mello, C. V., and Clayton, D. F. (1994). Song-induced ZENK gene expression in auditory pathways of songbird brain and its relation to the song control system. J. Neurosci. *14*, 6652–6666.

Mooney, R. (1992). Synaptic basis for developmental plasticity in a birdsong nucleus. J. Neurosci. *12*, 2464–2477.

Mooney, R., and Rao, M. (1994). Waiting periods versus early innervation: the development of axonal connections in the zebra finch song system. J. Neurosci. *14*, 6532–6543.

Morrison, R., and Nottebohm, F. (1993). Role of a telencephalic nucleus in the delayed song learning of socially isolated zebra finches. J. Neurobiol. *24*, 1045–1064.

Nakajo, S., Omato, K., Aiuchi, T., Shibayama, T., Okahashi, I., Ochiai, H., Nakai, Y., Nakaya, K., and Nakamura, Y. (1990). Purification and characterization of a novel brain-specific 14-kDa protein. J. Neurochem. *55*, 2031–2038.

Nakajo, S., Tsukada, K., Omata, K., Nakamura, Y., and Nakaya, K. (1993). A new brain-specific 14-kDa protein is a phosphoprotein: its complete amino acid sequence and evidence for phosphorylation. Eur. J. Biochem. *217*, 1057–1063.

Nakajo, S., Shioda, S., Nakai, Y., and Nakaya, K. (1994). Localization of phosphoneuroprotein 14 (PNP 14) and its mRNA expression in rat brain determined by immunocytochemistry and *in situ* hybridization. Mol. Brain Res. *27*, 81–86.

Nastiuk, K. L., and Clayton, D. F. (1995). The canary androgen receptor mRNA is localized in the song control nuclei of the brain and is rapidly regulated by testosterone. J. Neurobiol. *26*, 213–224.

Nastiuk, K. L., Mello, C. V., George, J. M., and Clayton, D. F. (1994). Immediate-early gene responses in the avian song control system: cloning and expression analysis of the canary c-jun cDNA. Mol. Brain Res. *27*, 299–309.

Nordeen, E. J., and Nordeen, K. W. (1990). Neurogenesis and sensitive periods in avian song learning. Trends Neurosci. *13*, 31–36.

Nordeen, E., Grace, A., Burek, M., and Nordeen, K. (1992). Sex-dependent loss of projection neurons involved in avian song learning. J. Neurobiol. *23*, 671–679.

Nottebohm, F. (1968). Auditory experience and song development in the Chaffinch, *Fringilla coelebs*. Ibis *110*, 549–568.

Nottebohm, F. (1981). A brain for all seasons: cyclical anatomical changes in song control nuclei of the canary brain. Science *214*, 1368–1370.

Nottebohm, F., Kelley, D. B., and Paton, J. A. (1982). Connections of vocal control nuclei in the canary telencephalon. J. Comp. Neurol. *207*, 344–357.

Represa, A., Deloulme, J. C., Sensenbrenner, M., Ben-Ari, Y., and Baudier, J. (1990). Neurogranin: immunocytochemical localization of a brain-specific protein kinase C substrate. J. Neurosci. *10*, 3782–3792.

Scharff, C., and Nottebohm, F. (1991). A comparative study of the behavioral deficits following lesions of various parts of the zebra finch

song system: implications for vocal learning. J. Neurosci. *11*, 2896–2913.

Segrest, J., Jackson, R., Morrisett, J., and Gotto, A. J. (1974). A molecular theory for protein–lipid interactions in plasma lipoproteins. FEBS Lett. *38*, 247–253.

Segrest, J., De Loof, H., Dohlman, J., Brouillette, C., and Anantharamaiah, G. (1990). Amphipathic helix motif: classes and properties. Proteins *8*, 103–117.

Segrest, J., Jones, M., De Loof, H., Brouillette, C., Venkatachalapathi, Y., and Anantharamaiah, G. (1992). The amphipathic helix in the exchangeable apolipoproteins: a review of secondary structure and function. J. Lipid Res. *33*, 141–166.

Shibayama-Imazu, T., Okahashi, I., Omata, K., Nakajo, S., Ochiai, H., Nakai, Y., Hama, T., Nakamura, Y., and Nakaya, K. (1993). Cell and tissue distribution and developmental change of neuron specific 14 kDa protein (phosphoneuroprotein 14). Brain Res. *622*, 17–25.

Shiffer, M., and Edmundson, A. (1967). Use of helical wheels to represent the structures of proteins and to identify segments with helical potential. Biophys. J. *7*, 121–135.

Sossinka, R., Prove, E., and Kalberlah, H. (1975). Der Einfluss von Testosteron auf den Gesangsbeginn beim Zebrafinken. Z. Tierpsychol. *39*, 259–264.

Thorpe, W. H. (1958). The learning of song patterns by birds, with especial reference to the song of the chaffinch, *Fringilla coelebs*. Ibis *100*, 535–570.

Tobe, T., Nakajo, S., Tanaka, A., Mitoya, A., Omata, K., Nakaya, K., Tomita, M., and Nakamura, Y. (1992). Cloning and characterization of the cDNA encoding a novel brain-specific 14-kDA protein. J. Neurochem. *59*, 1624–1629.

Towbin, H., Staehelin, T., and Gordon, J. (1979). Electrophoretic transfer of proteins from polyacrylamide gels to nitrocellulose sheets: procedure and some applications. Proc. Natl. Acad. Sci. USA *76*, 4350–4354.

Trimble, W. S., Linial, M., and Scheller, R. H. (1991). Cellular and molecular biology of the presynaptic nerve terminal. Annu. Rev. Neurosci. *14*, 93–122.

Ueda, K., Fukushima, H., Masliah, E., Xia, Y., Iwai, A., Yoshimoto, M., Otero, D., Kondo, J., Ihara, Y., and Saitoh, T. (1993). Molecular cloning of cDNA encoding an unrecognized component of amyloid in Alzheimer disease. Proc. Natl. Acad. Sci. USA *90*, 11282–11286.

Watson, J. B., Battenberg, E. F., Wong, K. K., Bloom, F. E., and Sutcliffe, J. G. (1990). Subtractive cDNA cloning of RC3, a rodent cortex-enriched mRNA encoding a novel 78 residue protein. J. Neurosci. Res. *26*, 397–408.

Wendland, B., Miller, K. G., Schilling, J., and Scheller, R. H. (1991). Differential expression of the p65 gene family. Neuron *6*, 993–1007.

Wiedenmann, B., and Franke, W. (1985). Identification and localization of synaptophysin, an integral membrane glycoprotein of M_r 38,000 characteristic of presynaptic vesicles. Cell *41*, 1017–1026.

GenBank Accession Number

The accession number for the synelfin sequence data presented in this paper is L33860.